Extended Abstracts of the 2013 International Conference on Solid State Devices and Materials, Fukuoka, 2013, pp984-985

K-1-4

Dark Current Reduction for GeSn p-i-n Photodetectors using Low-Temperature Si Passivation

Wei Wang,[1] Yuan Dong,[1] Genquan Han,[1] Pengfei Guo,[1] Xiao Gong,[1] Xin Xu,[1] Qian Zhou,[1] Lanxiang Wang,[1] Zhe Xu,[2] Wan-Khai Loke,[2] Soon-Fatt Yoon,[2] and Yee-Chia Yeo.[1,] *

[1] Department of Electrical and Computer Engineering, National University of Singapore (NUS), Singapore 117576.
[2] School of Electrical and Electronic Engineering, Nanyang Technological University, 50 Nanyang Avenue, Singapore 639798.
*Phone: +65 6516-2298, Fax: +65 6779-1103, E-mail: yeo@ieee.org

1. INTRODUCTION

Germanium-tin (GeSn) is an attractive material for the photodetectors (PDs) covering all telecommunication windows, due to its tunable bandgap [1]-[5]. However, the dark current of GeSn PDs is very high as compared with reported value of that of Ge and InGaAs-based PDs. The dark current of GeSn PDs is strongly dependent on the bulk and surface qualities of GeSn material. Therefore, improving these qualities is very important to realize GeSn PDs with low leakage current.

We have recently demonstrated that low-temperature Si passivation is effective for the surface passivation of GeSn pMOSFETs [6][7]. In this work, we report the first demonstration of GeSn PDs with Si surface passivation. A 75% reduction in surface leakage current density (J_{surf}) was achieved as compared to that of the PDs without Si passivation, and a minimum dark current of 1.5 μA at a bias of -1 V was demonstrated for a device with a diameter of 20 μm.

2. MATERIALS GROWTH AND CHARACTERIZATION

GeSn film was epitaxially grown at 170 °C by molecular beam epitaxy (MBE) on the n-type Ge(100) substrate with a resistivity of 0.01 to 0.03 Ω·cm. Fig. 1(a) shows the cross-sectional TEM image of a 780 nm-thick GeSn film on Ge(100). High resolution TEM image [Fig. 1(b)] depicts a good GeSn/Ge interface. High resolution XRD (004) and (224) curves show that the substitutional Sn composition is 2.6%, and the film is almost fully strained [Fig. 1(c)], with the degree of strain relaxation of ~3%. The full width at half maximum (FWHM) around (004) is 0.028°, indicating the high crystallinity of the $Ge_{0.974}Sn_{0.026}$ film.

3. DEVICE FABRICATION

The key process steps for fabricating a GeSn p-i-n PD are shown in Fig. 2(a). P-type contact layer was first formed by BF_2^+ implant and followed by thermal anneal at 400 °C for 30 minutes. The Raman spectra in Fig. 3 show that the lattice damage caused by BF_2^+ implant was not repaired completely, and some defects could remain in the surface layer.

After mesa formation, one sample was loaded into an ultra-high vacuum CVD system for native oxide removal by SF_6 plasma and 370 °C Si_2H_6 passivation to form a high quality and ultra-thin Si passivation layer. For the control sample, the Si passivation step was skipped. A 100 nm-thick SiO_2 layer was then deposited by sputter on both samples. Finally, top and bottom Al metal contacts were formed on GeSn and Ge surfaces, respectively. The PDs have mesa diameters ranging from 20 μm to 300 μm. Fig. 2(b) shows the schematic of a GeSn p-i-n PD, and Fig. 2(c) shows the top view SEM image of a device with a mesa diameter of 100 μm.

4. RESULTS AND DISCUSSION

The *I-V* characteristics of the GeSn PDs with and without Si passivation are shown in Fig. 4 and Fig. 5, respectively. A much lower dark current was achieved with Si passivation. For PDs with Si passivation, the diode currents are 1.5 μA and 18.8 μA at -1 V bias with a mesa diameter of 20 μm and 200 μm, which correspond to dark current densities of 478 mA/cm^2 and 59.9 mA/cm^2, respectively. The total dark current (I_{total}) is contributed from bulk leakage current (I_{bulk}) and surface leakage current (I_{surf}). To extract the bulk leakage current density (J_{bulk}) and the J_{surf} separately, numerical fitting was performed using

$$J_{total} = J_{bulk} + 4\ J_{surf}\ /D,$$

where $J_{total} = I_{total}$ /mesa area and D is the mesa diameter. Fig. 6 shows J_{total} versus 1/D at a bias of -2 V. Similar J_{bulk} of ~50 mA/cm^2 was extracted for devices with and without Si passivation. The low bulk current density confirms the high quality of the GeSn epitaxial layer. J_{surf} is reduced by 4 times for the devices with Si passivation, from 1.21 mA/cm to 0.3 mA/cm.

Photocurrents were measured using a tunable laser (1 mW) (Fig. 7 and Fig. 8). The light was aligned to the device mesa through an optical fiber, and the spot size was smaller than the active area of PDs. The photocurrents are similar for the PDs with and without Si passivation. At bias voltages of -3 V and -5 V, the photocurrents increase linearly with the laser power (Fig. 9). However, at -1 V bias, the photocurrent becomes saturated when the laser (1550 nm wave length) power is larger than 4 mW. Fig. 10 shows the responsivity versus diode bias at two different laser wavelengths. For the PDs with Si passivation, the responsivities at a -3 V bias are 0.45 A/W and 0.14 A/W, at laser wavelengths of 1550 and 1630 nm, respectively. This corresponds to external quantum efficiencies (EQEs) of 36% and 10.7%. Fig. 11 shows the responsivity spectrum (800-1650 nm) measured at a bias of -3 V by a halogen lamp combined with a monochromator. The responsivity spectrum was calibrated using the responsivity measured with a laser wavelength of 1550 nm to account for the inaccuracy caused by the bigger light spot size than the active area of PDs.

5. CONCLUSION

We demonstrate that the low-temperature Si passivation is effective for the surface passivation of GeSn PDs. J_{bulk} is low due to the high crystallinity of the GeSn epitaxial film, and J_{surf} is reduced by 4 times as compared with that of the PDs without Si passivation.

ACKNOWLEDGEMENT. The authors acknowledge support from the National Research Foundation under Grant NRF-CRP6-2010-4.

REFERENCES

[1] J. Mathews *et al.*, *APL* 95, 133506, 2009.
[2] J. Werner *et al.*, *APL* 98, 061108, 2011.
[3] S. J. Su *et al.*, *Optics Express* 19, 6400, 2011.
[4] M. Oehme *et al.*, *APL* 101, 141110, 2012.
[5] V. R. D'Costa *et al.*, *SST* 24, 115006, 2009.
[6] G. Han *et al.*, *IEDM 2011*, p. 402.
[7] X. Gong *et al.*,*VLSI Symp. 2012*, p. 99.

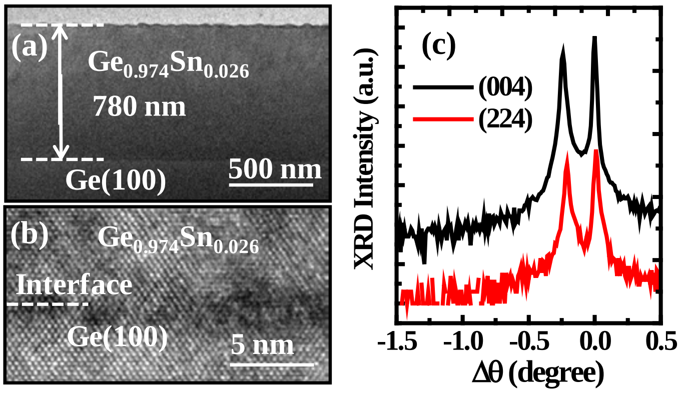

Fig. 1. (a) TEM image of GeSn film grown on Ge(100). (b) HRTEM image of interface region. (c) HRXRD (004) and (224) curves show that the GeSn film with a substitutional Sn composition of 2.6%.

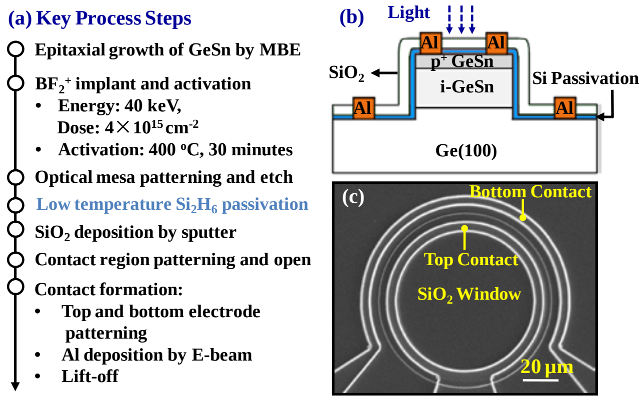

Fig. 2. (a) Key process steps used in the fabrication of GeSn p-i-n photodetector. (b) Schematic cross section and (b) top view SEM image of a GeSn p-i-n photodetector.

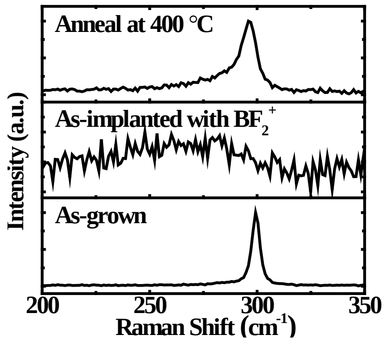

Fig. 3. Raman spectra from the as-grown, the as-implanted, and the post-implant annealed $Ge_{0.974}Sn_{0.026}$ films.

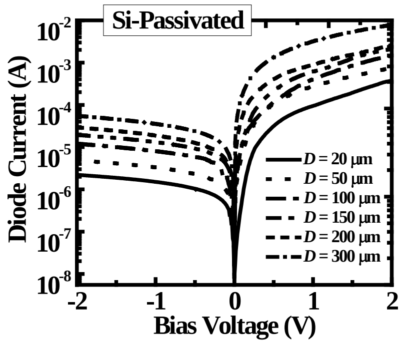

Fig. 4. Current-voltage (*I-V*) characteristics of the PDs without Si passivation.

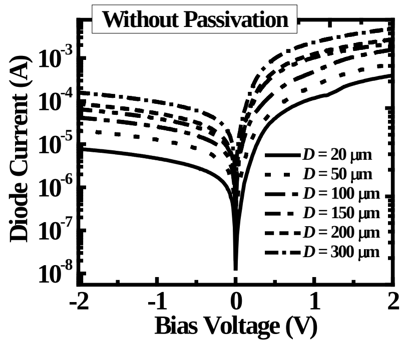

Fig. 5. Current-voltage (*I-V*) characteristics of the PDs with Si passivation.

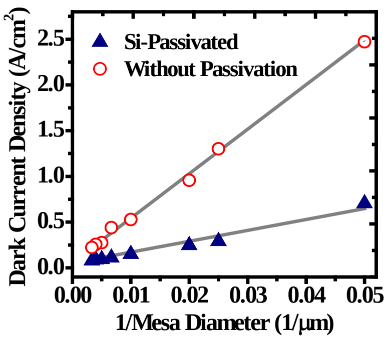

Fig. 6. Dark current density as a function of 1/Mesa Diameter at -2.0 V.

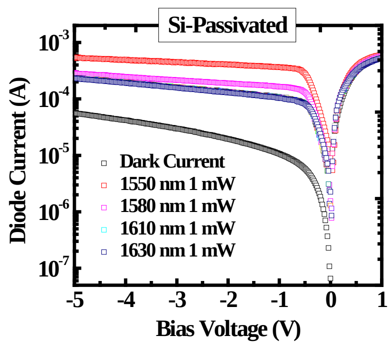

Fig. 7. *I-V* characteristics of the PDs with Si passivation under illumination.

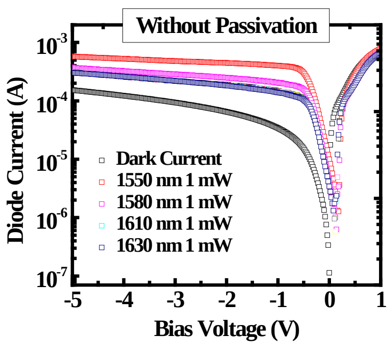

Fig. 8. *I-V* characteristics of the PDs without Si passivation under illumination.

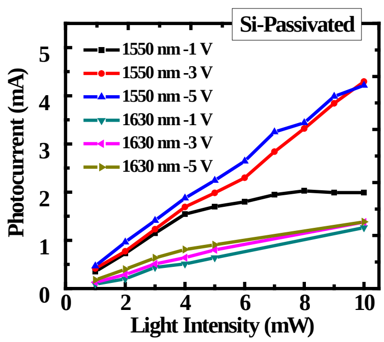

Fig. 9. Photocurrent as a function of the laser power at different biases.

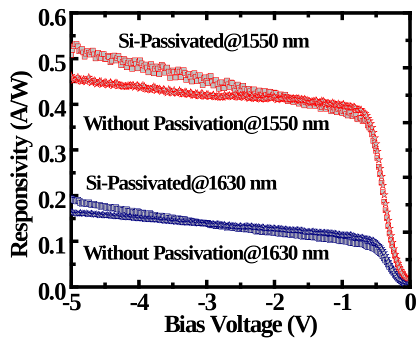

Fig. 10. Responsivity versus diode bias of the PDs with and without Si passivation.

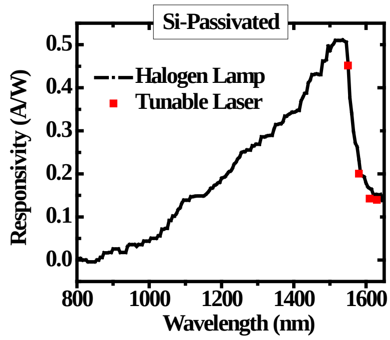

Fig. 11. Responsivity versus wavelength at -3 V bias.